

# Two Atoms in a Double Well: An Exact Solution

Yanxia Liu<sup>1</sup> and Yunbo Zhang<sup>1,\*</sup>

<sup>1</sup>*Institute of Theoretical Physics, Shanxi University, Taiyuan 030006, P. R. China*

We propose to experimentally realize an odd parity eigenstate  $|b\rangle$  of two atoms in the double well. The occupation probability of this state shows evident dependence on the interaction, distinct from the result of two-mode model adopted in the Heidelberg experiment. The tunneling dynamics of two atoms starting from the *NOON* state with infinite barrier height can be derived from the exactly solved model of  $\delta$ -barrier split double well based on a Bethe ansatz type hypothesis of the wave functions. We find that the single particle tunneling transfer the probabilities between double occupancy and single occupancy of each well.

PACS numbers: 03.75.Lm, 03.65.Ge, 67.85.De

**Introduction:** The deterministic preparation of few-particle systems makes it possible to study the tunneling of a few atoms out of a metastable state [1–3] or oscillation in double well [4, 5]. The double well is a typical model for the observation of Josephson oscillations in superconductor qubit [6, 7] and nonlinear self-trapping of Bose-Einstein condensates [8–10]. However, most studies so far relied on the two-mode model valid for sufficiently weak coupling [11, 12] or numerical methods for the dynamics [13–16].

Recently, the Heidelberg group has reported a new breakthrough in realizing two ultra-cold <sup>6</sup>Li fermionic atoms in an isolated double-well potential, which constitutes the fundamental building block of the Hubbard model at half filling [5]. In this experiment, the ground state  $|a\rangle$  and the excited state  $|c\rangle$  can be prepared with different interaction strength. The double occupancy of the two states is suppressed for increasing repulsive interactions. They did not bother to give the occupation statistics of the state  $|b\rangle$ , which are constants in the two-mode approximation. Practically tunneling of two atoms in a double well involves more single particle states and the occupation statistics of the state  $|b\rangle$  changes with interaction strength. The spatial wave functions of two fermions in a spin-singlet configuration  $|a\rangle$ ,  $|b\rangle$  and  $|c\rangle$  are symmetric with respect to particle exchange, which is identical to the case of two spinless bosons. On the other hand, the system has space inversion symmetry expressed as  $\Psi(x_1, x_2) = \pm\Psi(-x_1, -x_2)$  and the eigenstates can be classified into even parity with the sign “+” and odd parity with the sign “−”. The states  $|a\rangle$  and  $|c\rangle$  are even parity and the state  $|b\rangle$  is odd parity. The two-particle *NOON* state  $|b\rangle$  plays important role in several metrology proposals, including atomic frequency measurements [17], interferometry [18, 19], and matter-wave gyroscopes [20].

Motivated by the above experiment, in this Letter we choose the state  $|b\rangle$  as the initial state in double well and investigate the tunneling dynamics by an exactly solved model. There are a handful of exactly solved models in one dimension (1D), for instance, Lieb-Liniger model [21], Gaudin-Yang model [22, 23], etc [24]. Recent ex-

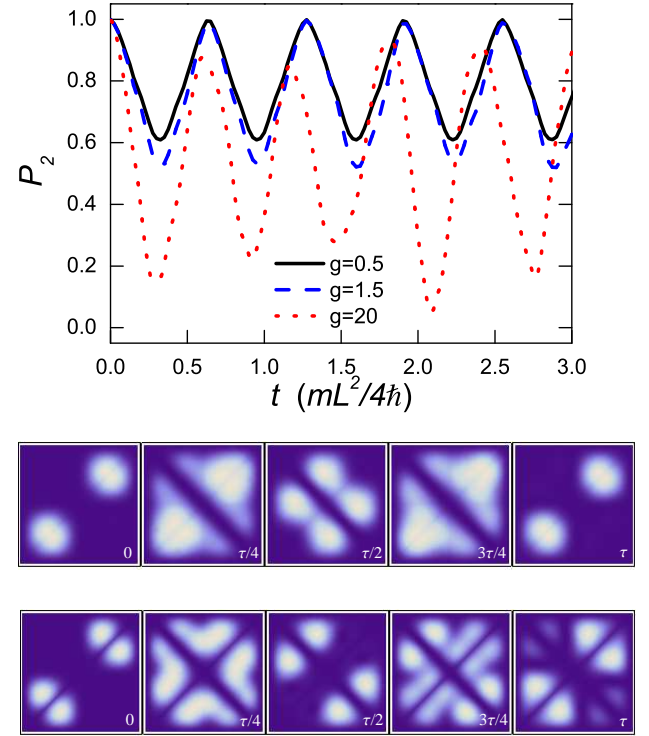


FIG. 1: (Color online). Top: Tunneling dynamics of the occupation probability  $P_2(t)$  of finding both atoms in the same well for  $g = 0.5$  (black solid line),  $g = 1.5$  (blue dashed line) and  $g = 20$  (red dotted line). The  $\delta$ -barrier is abruptly lowered from a height  $d = 300$  to  $0.5$  at time  $t = 0$ . Bottom: The two-body density functions  $\rho(x_1, x_2, t)$  at different times  $t$ , for  $g = 1.5$  and  $20$ , respectively.

periments on ultracold bosonic and fermionic atoms confined to 1D have provided a better understanding of the quantum statistical and dynamical effects in quantum many-body systems [25]. We give a new formulation on the exact solution of a  $\delta$ -split double well. Based on the analytically derived Bethe-ansatz-like equations and the Yang-Baxter-like relations for scattering matrices, we

propose a scheme to achieve accurate tunneling dynamics for two atoms in the *NOON* state of a double well as shown in Fig. 1.

*System:* We start with the model of  $N$  bosonic atoms of mass  $m$  confined in a 1D tube of length  $L$ , split by a  $\delta$ -function potential barrier at the center. The atoms interact through  $s$ -wave scattering and the Hamiltonian of the system can be written as

$$H = \sum_{i=1}^N \left[ -\frac{\hbar^2}{2m} \frac{\partial^2}{\partial x_i^2} + d\delta(x_i) + V(x_i) \right] + g \sum_{i < j}^N \delta(x_i - x_j), \quad (1)$$

where  $g$  is the interaction strength which can be tuned via magnetic Feshbach resonance and confinement induced resonance from  $-\infty$  to  $+\infty$ , and  $d > 0$  is the height of the  $\delta$ -function barrier. The square well  $V(x)$  with infinite depth is equivalent to the open boundary condition  $\Psi(x_i = \pm L/2) = 0, i = 1, 2, \dots, N$ , for the eigenfunction  $\Psi(x_1, x_2, \dots, x_N)$  of Hamiltonian  $H$ . The system in the absence of the  $\delta$ -barrier ( $d = 0$ ) reduces to the Lieb-Liniger model with open boundary conditions [26], while in the non-interacting case  $g = 0$  the problem turns out to be a single particle in split well. The system permits only solutions with odd parity as the situation when two particles simultaneously scatter on the  $d$ -barrier will not be considered here, just as the three-body interaction is omitted in Lieb-Liniger model. The addition of  $\delta$ -function barrier makes the system highly nontrivial and the ground-state properties of few-particle system in the split hard-wall potential have been examined in detail [15, 16] by means of the Bose-Fermi mapping in the Tonks-Girardeau limit and exact diagonalization method for finite interaction. Here we try to give an analytical solution in terms of Bethe's hypothesis and suitable connection conditions for wave functions.

The wave function is taken as the Bethe ansatz (BA) type

$$\begin{aligned} & \Psi(x_1, x_2, \dots, x_N) \\ &= \sum_{n=0}^N \sum_{Q, P} \sum_{\epsilon_P = \pm 1} \theta(x_{Q_1} < x_{Q_2} < \dots < x_{Q_N}) \\ & \quad \times A_n(Q, \epsilon_P P) \exp \left( i \sum_{l=1}^N \epsilon_{P_l} k_{P_l} x_{Q_l} \right), \end{aligned} \quad (2)$$

where  $Q = (Q_1, Q_2, \dots, Q_N)$  and  $P = (P_1, P_2, \dots, P_N)$  are two arrangements of  $(1, 2, \dots, N)$ . For the arrangement of the coordinates, we assume that  $n$  coordinates are less than 0, and the rest are larger than zero such that  $(x_{Q_1} < x_{Q_2} < \dots < x_{Q_n} < 0 < x_{Q_{n+1}} < \dots < x_{Q_N})$ . That is,  $n$  atoms are on the left side of the  $\delta$ -barrier and  $N - n$  of them are on the right side. We label such a block by a single index  $n$ , which is a square for  $N = 2$ , a cubic for  $N = 3$ , and so on. It constitutes of  $N!$  local regions in the sense of Lieb-Liniger model. The summation over  $n$

in Eq. (2) includes all possible  $N + 1$  blocks.  $\epsilon_P$  indicates that the particles move toward the right ( $\epsilon_P = +1$ ) or the left ( $\epsilon_P = -1$ ) and  $\theta$  is the step function. This system is featured by the fact that both interaction of two particles and the potential barrier are  $\delta$ -functions. Generally each  $\delta$ -function corresponds to a jump condition of the first derivative of wave function, which is used to connect adjoining regions. In presence of the potential barrier the momentum set  $\{k\}$  satisfy a series of transcendental equations, which play the role of BA equations [27]

$$ik_{P_n} \left( \frac{1 - R_{n-1}(P_n)}{1 + R_{n-1}(P_n)} - \frac{1 - R_n(P_n)}{1 + R_n(P_n)} \right) = \frac{2m}{\hbar^2} d, \quad (3)$$

with  $n, P_n = 1, 2, \dots, N$ . Here we define the reflection matrix  $R_{n-1}(P_n)$  as the ratio between coefficients  $A$  after and before the reverse of  $P_n$  in block  $n - 1$ , which reverses the sign of the momentum of the  $n$ -th particle

$$\begin{aligned} R_{n-1}(P_n) &= \frac{A_{n-1}(Q, \dots, -P_n, \dots)}{A_{n-1}(Q, \dots, P_n, \dots)} \\ &= -e^{ik_{P_n} L} \prod_{i=1}^{N-n} \frac{k_{P_{n+i}} - k_{P_n} + i\frac{m}{\hbar^2} g}{k_{P_{n+i}} - k_{P_n} - i\frac{m}{\hbar^2} g} \\ & \quad \times \frac{k_{P_{n+i}} + k_{P_n} - i\frac{m}{\hbar^2} g}{k_{P_{n+i}} + k_{P_n} + i\frac{m}{\hbar^2} g}. \end{aligned} \quad (4)$$

In a similar way  $R_n(P_n)$  inverses the momentum of the  $n$ -th particle in the block  $n$

$$\begin{aligned} R_n(P_n) &= \frac{A_n(Q, \dots, -P_n, \dots)}{A_n(Q, \dots, P_n, \dots)} \\ &= -e^{-ik_{P_n} L} \prod_{i=1}^{n-1} \frac{k_{P_n} - k_{P_{n-i}} + i\frac{m}{\hbar^2} g}{k_{P_n} - k_{P_{n-i}} - i\frac{m}{\hbar^2} g} \\ & \quad \times \frac{k_{P_n} + k_{P_{n-i}} + i\frac{m}{\hbar^2} g}{k_{P_n} + k_{P_{n-i}} - i\frac{m}{\hbar^2} g}. \end{aligned} \quad (5)$$

We note that the system is essentially the same when the number of atoms in the left well equals  $n$  or  $N - n$ . Due to this symmetry, there are altogether  $\frac{1}{2}N \sum_{j=0}^{N-1} C_{N-1}^j = 2^{N-2}N$  such BA-type equations. For  $d = 0$ , Eq. (3) is known as BA equation of the open boundary condition. When  $g = 0$ , Eq. (3) recovers the single particle result  $\tan(-k_{P_n} L/2 + \hbar^2 k_{P_n}/md) = 0$ .

In the scattering situation here the atoms preserve their momentum while changing their quantum internal states. The self-closed property of the system requires that the order of the collisions does not affect the final outcome. We find the Yang-Baxter equations (YBE)

$$\begin{aligned} & S_{d, P_n}(n+1) S_{d, P_{n+1}}(n) S_{P_n, P_{n+1}} \\ &= S_{P_n, P_{n+1}} S_{d, P_{n+1}}(n+1) S_{d, P_n}(n), \end{aligned} \quad (6)$$

which relies on the arrangement  $P$  and describes two equivalent processes from  $(d, P_n, P_{n+1})$  to  $(P_{n+1}, P_n, d)$ .

Often a solution of YBE is referred to as an scattering matrix. Here the scattering matrix between the  $d$ -barrier and the  $n$ -th particle is calculated as

$$\begin{aligned} S_{d,P_n}(n) &= \frac{A_n(Q, \dots, P_n, \dots)}{A_{n-1}(Q, \dots, P_n, \dots)} \\ &= \frac{1 + R_{n-1}(P_n)}{1 + R_n(P_n)}, \end{aligned} \quad (7)$$

which brings the system from block  $n - 1$  to  $n$ . The inverse scattering process is defined as  $S_{P_n,d}(n) = 1/S_{d,P_n}(n)$ , that is, the particle jumps from block  $n$  back to  $n - 1$ . The index  $n$  in the parentheses of  $S_{d,P_n}(n)$  indicates the position of  $P_n$  in the arrangement  $P$ . The L.H.S of Eq. (6) shows that firstly two neighboring particles scatter with each other in block  $n - 1$ , than scatter with the  $d$ -barrier in turn. The R.H.S of Eq. (6) shows that they scatter with the  $d$ -barrier first, then exchange their positions on the left of the  $d$ -barrier. The YBE is the basic algebraic constituent in the quantum inverse method and have been found in many model. The Eq. (6) is different from the regular YBE because there exist two distinct forms of scattering matrices [27]. Collisions of two adjacent particles in different blocks satisfy the same scattering matrix, so Eq. (6) is reduced to

$$S_{d,P_n}(n+1) S_{d,P_{n+1}}(n) = S_{d,P_{n+1}}(n+1) S_{d,P_n}(n). \quad (8)$$

The same equation holds for blocks  $n - 1$  and  $N - n + 1$  and in general there are  $\frac{1}{4}N(N-1) \sum_{j=0}^{N-2} C_{N-2}^j = N(N-1)2^{N-4}$  different equations for  $N > 2$ . When  $N = 2$ , there is only one such equation. The quasi-momentum  $k_i$  can be obtained by solving the sets of equations of (3) and (8) and the energy eigenvalue is  $E = \sum_{i=1}^N \frac{\hbar^2 k_i^2}{2m}$ .

*Tunneling dynamics in double-well:* We study the tunneling dynamics of two atoms in the double-well. Two interacting atoms are initially prepared in the  $NOON$  state  $|b\rangle$  of the double well with an infinite barrier height (numerically we set  $d = 300$ ). Then the barrier is abruptly lowered to a fixed height  $d = 0.5$ , which allows the atoms to tunnel between wells. Let the system evolve for different durations  $t$  and the resulting dynamics is observed by quickly increasing the barrier height, which freezes the spatial distribution of the atoms. One can then count the number of atoms in the left or right well by measuring their fluorescence. By implementing many of these measurements at different times, the time evolution of the probabilities can be determined experimentally.

The initial state in our proposed scheme is realized through solving Eq. (3) and Eq. (8) with the barrier height  $d = 300$  and plugging quasi-momentums  $k_1$  and  $k_2$  corresponding to the lowest energy into Eq. (2). This gives the initial state in the form  $|\phi_0(x_1, x_2)\rangle = (|LL\rangle - |RR\rangle)/\sqrt{2}$ , where  $|RR\rangle$  and

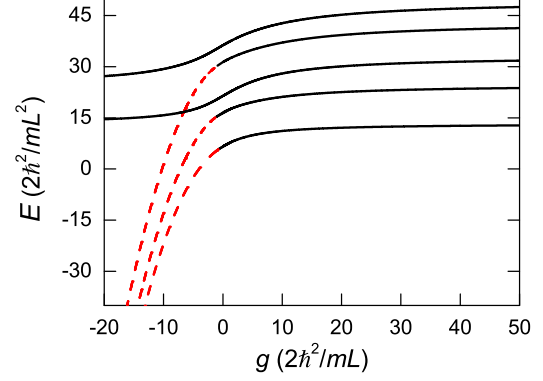


FIG. 2: (color online). Energy spectrum of two atoms in a double well. Five lowest eigenstates with odd parity in 1D split hard-wall potential are shown as a function of the interaction strength  $g$  for barrier height  $d = 0.5$ . The solid curves (black) show the eigenenergies of the bound states for atoms, the quasi-momentums of which are real numbers. The dashed curves (red) show those of the molecule states and the corresponding quasi-momentums are two conjugate complex numbers.

$|LL\rangle$  denote that both atoms reside in the ground state of the right or the left well. The correlation function, also known as the two-body density, is defined as  $\rho(x_1, x_2, t) = \phi^*(x_1, x_2, t)\phi(x_1, x_2, t)$ . Starting from the initial state  $|\phi_0(x_1, x_2)\rangle$ , the time evolution of the wave function is governed by  $|\phi(x_1, x_2, t)\rangle = e^{-\frac{i}{\hbar}Ht}|\phi_0(x_1, x_2)\rangle = \sum_i C_i e^{-\frac{i}{\hbar}E_i t}|\Psi_i(x_1, x_2)\rangle$ , in which  $C_i = \langle\Psi_i(x_1, x_2)|\phi_0(x_1, x_2)\rangle$  is the overlap of the initial state and the  $i$ -th eigenstate of the system  $\Psi_i(x_1, x_2)$  with eigen energy  $E_i$  for barrier height  $d = 0.5$ . The correlation function can be calculated as

$$\begin{aligned} \rho(x_1, x_2, t) &= \sum_{i=1} |C_i \Psi_i(x_1, x_2)|^2 + \sum_{i < j} 2C_i C_j \\ &\quad \times \Psi_i(x_1, x_2) \Psi_j(x_1, x_2) \cos[(E_i - E_j)t/\hbar]. \end{aligned} \quad (9)$$

We introduce in theory the probabilities of finding  $n$  particles in the right or left well as  $P_{Rn}(t)$  and  $P_{Ln}(t)$ . The system remains population balanced at any subsequent time and it will be as likely to find both atoms in the same well as in the opposite one, i.e.  $P_{Rn}(t) = P_{Ln}(t)$ . The mean particle number in right well is  $\bar{N}(t) = 2P_{R2}(t) + P_{R1}(t)$ , which is a constant with the population-balanced initial state and equals to 1. Then the probability of finding both particles in the same well is  $P_2(t) = 2P_{R2}(t) = 2 \int_0^{L/2} \int_0^{L/2} \rho(x_1, x_2, t) dx_1 dx_2$  and that in different wells is  $P_1(t) = P_{R1}(t) = 2 \int_{-L/2}^0 \int_0^{L/2} \rho(x_1, x_2, t) dx_1 dx_2$  [13]. We emphasize that the pair tunneling between double wells cancel each other in our system, while the single

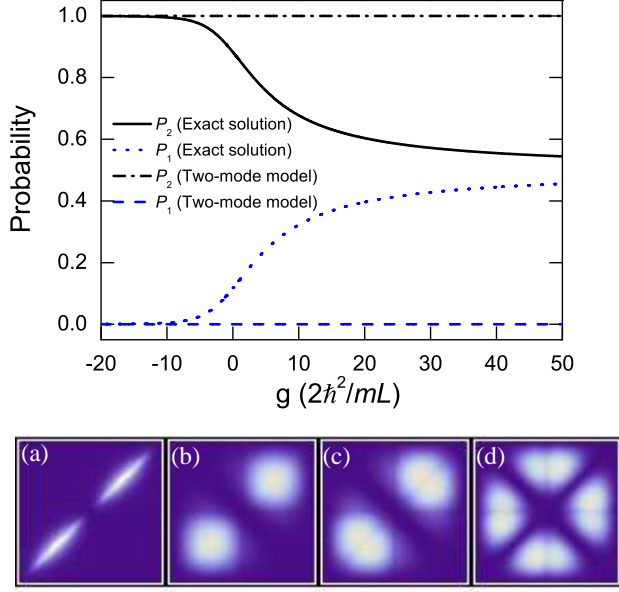


FIG. 3: (Color online). Top: Occupation probabilities as a function of the interaction strength. The relative probabilities of both particles in the same well ( $P_2$ , black curves) or in different wells ( $P_1$ , blue curves) are shown. The solid and dotted lines show the results of our exact solution. The dash-dotted and dashed curves show the those of two-mode model. Bottom: The two-body density  $\rho(x_1, x_2)$  of the state  $|b\rangle$  for different interaction strengths (a)  $g = -10$ , (b)  $g = -0.5$ , (c)  $g = 1.5$  and (d)  $g = 50$ .

particle tunneling will transfer the probabilities between double occupancy  $P_2(t)$  and single occupancy  $P_1(t)$ .

To better understand the oscillations in the probability, Fig. 2 presents the evolution of the two-body eigen energies  $E_i$  as  $g$  is varied. In Fig. 2, we plot results of the spectrum for case  $d = 0.5$ . Due to the odd symmetry of the initial state  $|b\rangle$ , what we need in the time evolution are only those states with odd parity. Note that the quasi-momentums of the bound states of atoms  $\Psi(x_1, x_2)$  are real number, while those of the molecule states are two conjugate complex numbers in the form of  $k_{1,2} = \alpha \pm i\Lambda$ , which only happen for  $g < 0$ . As we can see in the Eq. (9), the oscillation frequencies of the particles in double well are related to the energy differences  $\Delta E_{ij} = E_i - E_j$ . Through calculating weight coefficients  $C_i$ , we find that the first few  $\Psi_i$ 's make most important contribution to the time evolution of correlation function  $\rho(x_1, x_2, t)$ .

We propose here to experimentally realize the state  $|b\rangle$  and measure the influence of the interaction strength on the distribution of the two particles between the wells. The occupation probability of the eigenstate  $|b\rangle = \Psi_1(x_1, x_2)$ , which is nothing but the lowest energy level in Fig. 2, is given in Fig. 3. Together shown are the

two-body density  $\rho_1(x_1, x_2)$  for four typical values of  $g$  with  $d = 0.5$ . There exists a big difference between the results of two-mode model and our exact solution. Both the double occupancy and single occupancy probabilities of the state  $|b\rangle$  are constants in two-mode model. Clearly two-mode model is not any more a good choice for double well, especially when the interaction between two particles is strong or the excited states are involved in the tunneling dynamics. Our calculation based on the exactly solved model predict drastically different result: the double occupancy is suppressed for increasing repulsive interactions, however, unlike in the case of ground state  $|a\rangle$ , to an asymptotic value of 50%. The single occupancy probability, on the other hand, is enhanced to 50% for strong repulsion. The probabilities of double occupancy  $P_2$  and single occupancy  $P_1$  tend towards equalization, which occurs in the experiment [5] for the ground state  $|a\rangle$  and excited state  $|c\rangle$  of the non-interacting system. Attractive interaction prefers the two atoms forming a molecule with large binding energy, which will extinguish the probability of single particle tunneling and double occupancy would dominate. The system approaches the two-particle analog of a charge-density-wave state. The state  $|b\rangle$  is the two-particle *NOON* state, only when the attractive interaction is large (an example is shown in Fig. 3(a)) or the barrier height  $d$  is infinity [27]. The wave function of the odd parity symmetry state  $|b\rangle$  is anti-symmetric about the nodal line  $x_1 = -x_2$ . From the corresponding two-body density patterns shown in the bottom of Fig 3, we see that for a fixed value of  $d$  the density for molecular states in attractive interaction has two peak values along the diagonal line  $x_1 = x_2$ . In the case of repulsive interaction the probability accumulates gradually to the single occupancy region and finally the probabilities  $P_1$  and  $P_2$  are equally distributed in the strong interaction limit.

In order to explore the physical phenomenon behind the tunneling dynamics, we investigate the effect of the interaction strength  $g$  on oscillation of the double occupancy probability  $P_2(t)$  as shown in Fig. 1. We choose 30 eigenstates  $\Psi_i(x_1, x_2)$  as the basis states to study the tunneling dynamics, since the weight coefficients  $C_i$  are very small, when  $i > 30$ . The time evolution of  $P_2(t)$  is illustrated in Fig. 1 for repulsive interaction strengths from weak to strong. The atoms tunnel back and forth between the double well, as a result the probabilities  $P_2$  oscillate with time and the amplitude increases with  $g$  due to the enhancement of the tunneling rate. Stronger repulsion will destroy the perfect oscillation such that the double occupancy probability in the initial *NOON* state can not be retrieved with 100% fidelity. The oscillation period shrinks from  $\tau = 0.64$  for  $g = 1.5$  to  $\tau = 0.6$  for  $g = 20$ . The two-body density in the bottom of Fig. 1 shows that the probability will be redistributed in blocks  $n = 0, 2$  and 1, leaving partial residual probability after the completion of an oscillation.

Experimental realization of our  $\delta$ -split double well includes producing the quasi-1D waveguide and loading two atoms in the motional ground state of a single optical microtrap. A cylindrically focused blue-detuned Gaussian laser beam directed perpendicular to the long axis of the confining potential is used to cut the waveguide in half [28]. A series of such laser beams with equal spatial distance create a lattice model. Moreover, the ability of preparing the two atoms in the excited states  $|b\rangle$  and  $|c\rangle$  allows for a direct realization of population of higher bands, which contains the physics responsible for the formation of novel ordered phases in many-body system [29, 30].

*Conclusions:* We present the Bethe-ansatz type exact solution for  $N$  interacting bosonic atoms in the  $\delta$ -split double well, the result of which for two atoms are applied to the tunneling dynamics starting from an odd parity state  $|b\rangle$ . The occupation probability show evident dependence on the interaction and tend towards 50% – 50% equalization which is different from the result of two-mode model adopted in the experiment. The probabilities are found to oscillate between double and single occupancy in the tunneling dynamics.

This work is supported by NSF of China under Grant Nos. 11234008 and 11474189, the National Basic Research Program of China (973 Program) under Grant No. 2011CB921601, Program for Changjiang Scholars and Innovative Research Team in University (PCSIRT)(No. IRT13076).

---

\* Electronic address: ybzhang@sxu.edu.cn

- [1] G. Zürn, F. Serwane, T. Lompe, A. N. Wenz, M. G. Ries, J. E. Bohn, and S. Jochim, Phys. Rev. Lett. **108**, 075303 (2012).
- [2] M. Rontani, Phys. Rev. Lett. **108**, 115302 (2012).
- [3] G. Zürn, A. N. Wenz, S. Murmann, A. Bergschneider, T. Lompe, S. Jochim, Phys. Rev. Lett. **111**, 175302 (2013).
- [4] P. Cheinet, S. Trotzky, M. Feld, U. Schnorrberger, M. Moreno-Cardoner, S. Fölling, and I. Bloch, Phys. Rev. Lett. **101**, 090404 (2008).
- [5] S. Murmann, A. Bergschneider, V. M. Klinkhamer, G. Zürn, T. Lompe, and S. Jochim, (2014), arXiv:1410.8784v1.
- [6] K. B. Cooper, M. Steffen, R. McDermott, R. W. Simmonds, Seongshik Oh, D. A. Hite, D. P. Pappas, and John M. Martinis, Phys. Rev. Lett. **93**, 180401 (2004).
- [7] R. W. Simmonds, K. M. Lang, D. A. Hite, S. Nam, D. P. Pappas, and J. M. Martinis, Phys. Rev. Lett. **93**, 077003 (2004).
- [8] M. Albiez, R. Gati, J. Fölling, S. Hunsmann, M. Cristiani, and M. K. Oberthaler Phys. Rev. Lett. **95**, 010402 (2005).
- [9] Y. Shin, M. Saba, T. A. Pasquini, W. Ketterle, D. E. Pritchard, and A. E. Leanhard, Phys. Rev. Lett. **92**, 050405 (2004).
- [10] M. Saba, T. A. Pasquini, C. Sanner, Y. Shin, W. Ketterle, and D. E. Pritchard, Science **307**, 1948 (2005).
- [11] G. J. Milburn, J. Corney, E. M. Wright, and D. F. Walls, Phys. Rev. A **55**, 4318 (1997).
- [12] A. Smerzi, S. Fantoni, S. Giovanazzi, and S. R. Shenoy, Phys. Rev. Lett. **79**, 4950 (1997).
- [13] S. Zöllner, H.-D. Meyer, and P. Schmelcher, Phys. Rev. Lett. **100**, 040401 (2008).
- [14] D. S. Murphy, J. F. McCann, J. Goold, and Th. Busch, Phys. Rev. A **76**, 053616 (2007).
- [15] X. Yin, Y. Hao, S. Chen, and Y. Zhang, Phys. Rev. A **78**, 013604 (2008).
- [16] X. Lü, X. Yin, and Y. Zhang, Phys. Rev. A **81**, 043607 (2010).
- [17] J. J. Bollinger, W. M. Itano, D. J. Wineland, and D. J. Heinzen, Phys. Rev. A **54**, R4649 (1996).
- [18] M. J. Holland and K. Burnett, Phys. Rev. Lett. **71**, 1355 (1993).
- [19] R. A. Campos, C. C. Gerry, and A. Benmoussa, Phys. Rev. A **68**, 023810 (2003).
- [20] J. P. Dowling, Phys. Rev. A **57**, 4736 (1998).
- [21] E. H. Lieb, and W. Liniger, Phys. Rev. **130**, 1605 (1963).
- [22] M. Gaudin, Phys. Lett. A **24**, 55 (1967).
- [23] C. N. Yang, Phys. Rev. Lett. **19**, 1312 (1967).
- [24] M. Takahashi, Thermodynamics of One Dimensional Solvable Models (Cambridge University Press, Cambridge, England, 1999).
- [25] X. W. Guan, M. T. Batchelor, C. H. Lee, Rev. Mod. Phys. **85**, 1633 (2013).
- [26] Y. Hao, Y. Zhang, J.-Q. Liang and S. Chen, Phys. Rev. A **73**, 063617 (2006).
- [27] See Supplemental Material.
- [28] J. H. V. Nguyen, P. Dyke, D. Luo, B. A. Malomed and R. G. Hulet, Nat. Phys. 10.1038/nphys3135
- [29] T. Müller, S. Fölling, A. Widera, and I. Bloch, Phys. Rev. Lett. **99**, 200405 (2007).
- [30] G. Wirth, M. Ölschläger, and A. Hemmerich, Nat. Phys. **7**, 147 (2011).

# Supplementary Material of Two Atoms in a Double Well: an Exact Solution

Yanxia Liu<sup>1</sup> and Yunbo Zhang<sup>1,\*</sup>

<sup>1</sup>*Institute of Theoretical Physics, Shanxi University, Taiyuan 030006, P. R. China*

PACS numbers: 03.75.Lm, 03.65.Ge, 67.85.De

## Appendix A: Bethe-ansatz-type equations

Here we show the details on how to exactly solve the system of interacting  $N$  particles in the 1D  $\delta$ -barrier split double well. For this system, the key to the exact solution is region allocation. Denote the configuration of  $n$  particles in the left well as block  $n$ . We connect the adjacent regions in a fixed block  $n$ , and then connect the blocks  $n$  and  $n-1$  step by step. Take the two particles case as an example. We can transform the two-particle 1D problem into a 2D problem of one particle, as shown in Fig. 1. We divide the  $x_1x_2$  box into six regions. The regions I and II constitute block 0, region III and VI constitute block 1 and IV and V constitute block 2. Detailed analysis procedure of the  $N$  particle cases is demonstrated below. For bosons the wave function of the system is symmetric under coordinates exchange

$$\Psi(\cdots x_i, \cdots x_j \cdots) = \Psi(\cdots x_j, \cdots x_i \cdots), \quad (\text{A1})$$

which means

$$A_n(Q, \epsilon_P P) = A_n(Q', \epsilon_P P). \quad (\text{A2})$$

Thus for fixed  $n$  the coefficients are equal for all local regions assigned by arrangements  $Q' = (Q'_1, Q'_2, Q'_3, \cdots, Q'_N)$ . In this block, we noticed that the open boundary conditions are imposed on the left end of the tube

$$\Psi\left(x_{Q_i} = -\frac{L}{2}\right) = 0, i = 1, 2, \cdots n, \quad (\text{A3})$$

for particles in the left side and on the right end

$$\Psi\left(x_{Q_i} = \frac{L}{2}\right) = 0, i = n+1, \cdots N. \quad (\text{A4})$$

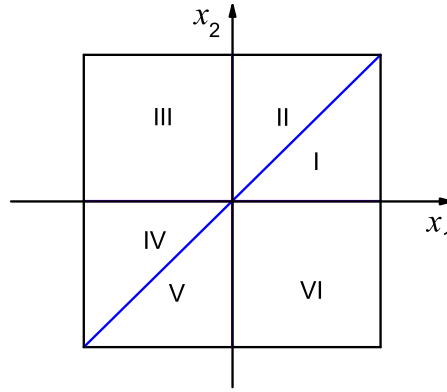


FIG. 1: (Color online). The square well with infinite depth can be dissolved into six regions by the  $x_1$  axis,  $x_2$  axis, and the line  $x_1 = x_2$ . The adjacent regions are connected by the continuous conditions of wave functions and jump conditions of the first derivative of wave functions. Away from these lines, the particles are free.

---

\*Electronic address: ybzhzhang@sxu.edu.cn

for particles in the right well. We define the reflection matrix  $R(P_1)$

$$R(P_1) = \frac{A_n(Q, -P_1, \dots, \epsilon_{P_N} P_N)}{A_n(Q, P_1, \dots, \epsilon_{P_N} P_N)} = -\exp(-ik_{P_1} L), \quad (\text{A5})$$

and  $R(P_N)$

$$R(P_N) = \frac{A_n(Q, \epsilon_{P_1} P_1, \dots, -P_N)}{A_n(Q, \epsilon_{P_1} P_1, \dots, P_N)} = -\exp(ik_{P_N} L). \quad (\text{A6})$$

Two special cases are that all particles are located on the right or left side of the barrier such that we have only half of the boundary condition (A4) or (A3). Thus only the reflection matrix  $R(P_N)$  or  $R(P_1)$  survives for block  $n = 0$  or  $N$ , respectively, and only the rightmost or leftmost atom can be reflected on the boundaries and get a phase shift.

Next we discuss the scattering between two particles. Let  $x_i$  and  $x_j$  be coordinates of two adjacent particles in the same side of the barrier. Particles in different well cannot collide with each other. In the relative coordinates the first derivative of wave function is not continuous due to the  $g$ -interaction,

$$\left[ \left( \frac{\partial \Psi}{\partial x_i} - \frac{\partial \Psi}{\partial x_j} \right) |_{x_i - x_j = 0} \right] - \frac{m}{\hbar^2} g \Psi |_{x_i - x_j = 0} = 0,$$

which connects different local regions in one block. Generally there are  $N(N-1)/2$  such equations in each block and they are equivalent to each other for different blocks. One exceptional case is  $N = 2$ : we have one equation for blocks  $n = 0$  or  $2$ , while no  $g$ -interaction condition in block  $n = 1$ . In a similar way we define the scattering matrix  $S_{\epsilon_{P_i} P_i, \epsilon_{P_j} P_j}$  describing the elastic collision between the two particles

$$\begin{aligned} S_{\epsilon_{P_i} P_i, \epsilon_{P_j} P_j} &= \frac{A_n(Q, \dots, \epsilon_{P_j} P_j, \epsilon_{P_i} P_i, \dots)}{A_n(Q, \dots, \epsilon_{P_i} P_i, \epsilon_{P_j} P_j, \dots)} \\ &= \frac{\epsilon_{P_i} k_{P_i} - \epsilon_{P_j} k_{P_j} - i \frac{m}{\hbar^2} g}{\epsilon_{P_i} k_{P_i} - \epsilon_{P_j} k_{P_j} + i \frac{m}{\hbar^2} g}. \end{aligned} \quad (\text{A7})$$

The matrices  $R(P_1)$ ,  $R(P_N)$  and  $S_{\epsilon_{P_i} P_i, \epsilon_{P_j} P_j}$  are defined in the same way as in Lieb-Liniger model with hard wall boundary conditions. The missing reflection and scattering matrices make it impossible to get the Bethe ansatz equation in a single block  $n$ . We shall see in the following, the jump conditions between blocks with different  $n$  play essential role in the exact solution of our model.

The jump condition due to the  $d$ -barrier at  $x_{Q_n} = 0$  connects the blocks  $n-1$  and  $n$ , which can be obtained by integrating the Schrödinger equation from  $x_{Q_n} = 0_-$  to  $x_{Q_n} = 0_+$

$$\left[ \frac{\partial \Psi}{\partial x_{Q_n}} |_{x_{Q_n}=0_+} - \frac{\partial \Psi}{\partial x_{Q_n}} |_{x_{Q_n}=0_-} \right] - \frac{2m}{\hbar^2} d \Psi |_{x_{Q_n}=0} = 0. \quad (\text{A8})$$

It means that the  $n$ -th particle jumps from the right to the left. Inserting the Bethe-ansatz wave function Eq. (2) into Eq. (A8), we get the relation

$$\begin{aligned} &\left( ik_{P_n} - \frac{m}{\hbar^2} d \right) A_{n-1}(Q, \dots, P_n, \dots) \\ &- \left( ik_{P_n} + \frac{m}{\hbar^2} d \right) A_{n-1}(Q, \dots, -P_n, \dots) \\ &- \left( ik_{P_n} + \frac{m}{\hbar^2} d \right) A_n(Q, \dots, P_n, \dots) \\ &+ \left( ik_{P_n} - \frac{m}{\hbar^2} d \right) A_n(Q, \dots, -P_n, \dots) = 0. \end{aligned} \quad (\text{A9})$$

Seemingly cumbersome, this is a basic relationship between four coefficients  $A$  in blocks  $n-1$  and  $n$ . Through the above analysis, we know that to reverse the sign of the  $n$ -th particle's momentum in block  $n-1$ , the particle needs firstly to scatter with the right neighboring atoms for  $N-n$  times until there are no more atoms to scatter, then reflect on the boundary and finally scatter with the left neighboring atoms for the same times. This successive scattering process will reverse the sign of  $P_n$  and by repeatedly using the matrices  $S_{\epsilon_{P_i} P_i, \epsilon_{P_j} P_j}$  and  $R(P_N)$  we can get the Eq. (4). Note that  $R_{n-1}(P_n) = R(P_N)$  for  $n = N$ . In a similar way we can inverse the momentum of the  $n$ -th particle in the block  $n$  by moving first toward left, reflecting on the boundary  $-L/2$  and going back to its original position



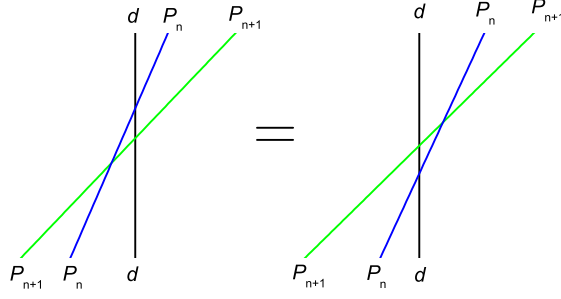


FIG. 2: (Color online). Graphical representation of two possible ways of two particles scattering with  $d$ -barrier.

toward right. This gives the Eq. (5). Similarly we have  $R_n(P_n) = R(P_1)$  for  $n = 1$ . In Eq. (A9) we replace the coefficients  $A$  with  $-P_n$  by their counterpart with  $P_n$  through Eq. (4) and Eq. (5) and the scattering matrix between the  $d$ -barrier and the  $n$ -th particle is calculated as

$$\begin{aligned} S_{d,P_n}(n) &= \frac{A_n(Q, \dots, P_n, \dots)}{A_{n-1}(Q, \dots, P_n, \dots)} \\ &= \frac{ik_{P_n}(1 - R_{n-1}(P_n)) - \frac{m}{\hbar^2}d(1 + R_{n-1}(P_n))}{ik_{P_n}(1 - R_n(P_n)) + \frac{m}{\hbar^2}d(1 + R_n(P_n))}, \end{aligned} \quad (\text{A10})$$

which brings the system from block  $n - 1$  to  $n$ . The continuous condition of wave function  $\Psi|_{x_{Q_n}=0+} = \Psi|_{x_{Q_n}=0-}$ , on the other hand, gives an alternative form of this scattering matrix with  $d$ -barrier, that is, Eq. (7). Then we infer that in presence of the potential barrier the momentum set  $\{k\}$  satisfy the BA-type equations (3). For  $N = 2$ , the BA-type equation can be written as

$$ik_1 \left( \frac{1 + \frac{k_2 - k_1 + i\frac{m}{\hbar^2}g}{k_2 - k_1 - i\frac{2\mu}{\hbar^2}g} \cdot \frac{k_2 + k_1 - i\frac{m}{\hbar^2}g}{k_2 + k_1 + i\frac{m}{\hbar^2}g} \exp(ik_1 L)}{1 - \frac{k_2 - k_1 + i\frac{m}{\hbar^2}g}{k_2 - k_1 - i\frac{2\mu}{\hbar^2}g} \cdot \frac{k_2 + k_1 - i\frac{m}{\hbar^2}g}{k_2 + k_1 + i\frac{m}{\hbar^2}g} \exp(ik_1 L)} - \frac{1 + \exp(-ik_1 L)}{1 - \exp(-ik_1 L)} \right) = \frac{2m}{\hbar^2}d. \quad (\text{A11})$$

Another BA-type equation can be obtained by swapping the positions of  $k_1$  and  $k_2$ .

## Appendix B: Yang-Baxter-Type relation

Since Yang and Baxter's pioneering works, the quantum Yang-Baxter equation (QYBE), which define the underlying algebraic structure, has become a cornerstone for constructing and solving the integrable models. Yang-Baxter-Type relation (6) can be represented graphically. In Fig. 2 we show two equivalent scattering ways of two particles with the barrier. The black vertical line indicates that the barrier is localized in the center. Each intersection between two lines is represented by a scattering matrix. The arrow of time is taken from top to bottom. There are two distinct forms of S-matrix, that between particles and that between the particle and the barrier. For  $N = 2$ , Eq. (8) can be written as

$$\begin{aligned} &\sin^2\left(\frac{k_1 L}{2}\right) \sin^2\left(-\arctan\left(\frac{\frac{m}{\hbar^2}g}{k_1 + k_2}\right) + \arctan\left(\frac{\frac{m}{\hbar^2}g}{k_1 - k_2}\right) + \frac{k_2 L}{2}\right) \\ &= \sin^2\left(\frac{k_2 L}{2}\right) \sin^2\left(-\arctan\left(\frac{\frac{m}{\hbar^2}g}{k_1 + k_2}\right) - \arctan\left(\frac{\frac{m}{\hbar^2}g}{k_1 - k_2}\right) + \frac{k_1 L}{2}\right) \end{aligned} \quad (\text{B1})$$

## Appendix C: The energy spectrum for two particles in a double well

The energy spectrum for two particles in a double well is obtained by numerically solving the three transcendental equations Eq. (A11) and Eq. (B1) for given barrier height  $d$ . In Fig. 3, we plot the energy spectrum as a function of  $g$  for limiting case  $d = 0$  and a moderate barrier height  $d = 2$ . In the absence of  $\delta$ -function potential barrier we



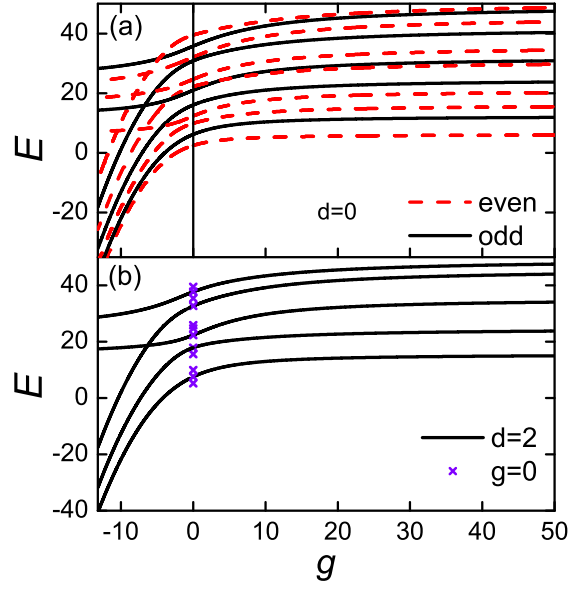


FIG. 3: (Color online). The energy spectrum for the system of particles in 1D square well with infinite depth (a)  $d = 0$  and particles in 1D split hard-wall potential (b)  $d = 2$ . The  $\times$  signs indicate the energy for  $g = 0$ . The (red) dash lines show the spectrum for even parity states. The (black) solid lines show the spectrum for odd parity states.

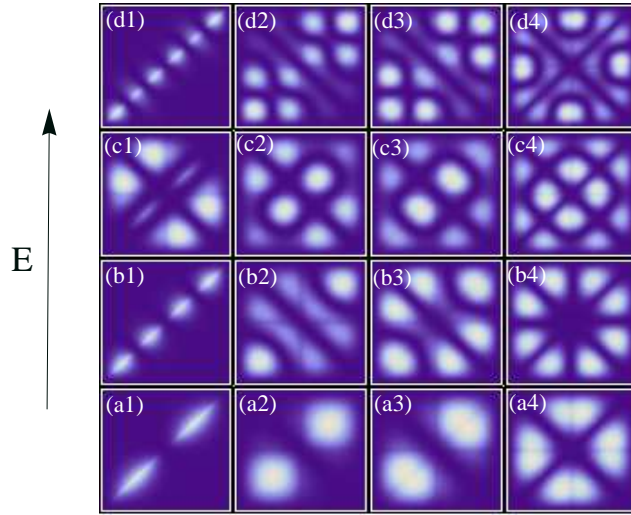


FIG. 4: (Color online). The normalized probability density  $\rho(x_1, x_2)$  for two particles in a double-well potential with  $d = 2$  for different  $g$ . The columns represent results for four interaction parameters  $g = -6.295, -0.5, 1.5, 50$ , respectively. From bottom to up the rows are for four lowest states. Each individual plot spans the range  $-1 < x_1, x_2 < 1$ .

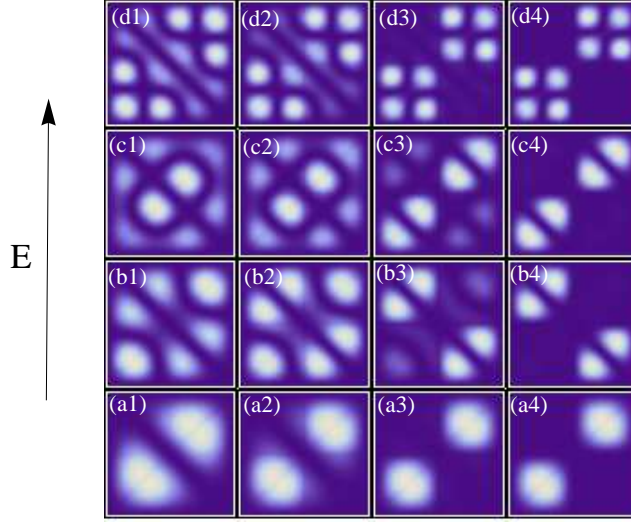


FIG. 5: (Color online). The normalized probability density  $\rho(x_1, x_2)$  for two particles in a double-well potential for  $g = 1.5$  with different  $d$ . The columns represent results for four barrier height  $d = 0.5, 1.5, 10, 50$ , respectively. From bottom to up the rows are for four lowest states. Each individual plot spans the range  $-1 < x_1, x_2 < 1$ .

find two kinds of parity symmetry bound states [see Fig. 3(a)], while there are only odd parity bound states for finite potential barrier [Fig. 3(b)] except at  $g = 0$ . Note a level crossing between the bound state of atoms and the molecular state occurs at  $g = -6.295$ .

The two-body density  $\rho(x_1, x_2)$  for a fixed barrier height  $d = 2$  is presented in Fig. 4. From the ground state density in first row of Fig. 4 (a1-a4) we see almost no difference with a lower barrier  $d = 0.5$ . Again as in Fig. 4 in the main text we choose four typical interaction strength parameters  $g = -6.295, -0.5, 1.5, 50$ , one of which is exactly the level crossing point. There we see that for a fixed value of  $d$ , the densities for molecular states reside along the diagonal line  $x_1 = x_2$ . For repulsive interactions, the probability of double occupancy is transferred into the single occupancy region as  $g$  increases and the two finally reach equalization for strong interaction. The two-body densities for higher excited states in Fig. 4 (b-d) show more bizarre oscillations and more nodal lines divided the plane into small probability islands, unveiling an equal distribution of the double and single occupancy probability for strong repulsive interaction. We also note the big difference for the molecular state and the atomic state. While there are always probability for the single occupancy in the atomic states, the molecular state tend to exclude it. An typical example is shown in panels (c1) and (d1).

Fig. 5 shows the two-body density  $\rho(x_1, x_2)$  with a fixed value  $g = 1.5$  for different  $d$ . In the lowest odd symmetry state the density tends to converge towards the first and third quadrants and the probability of double occupancy  $P_2$  is approaching 1 as  $d$  increases, which eventually achieves the *NOON* state in (a4). While we observe similar tendency for the third and the fourth states, the density of the some higher excited states (the second one in Fig. 5(b1-b4), also the fifth one which is not shown) exhibits opposite behavior, which tends to converge towards the second and fourth quadrants and probability  $P_2$  is approaching 0 for higher barrier. The excited states are classified according to the total energy of both atoms proportional to  $k_1^2 + k_2^2$ . In extreme case of  $g = 0$  with very high barrier, (a4) and (d4) reduce to the states with almost equal quasi-momentum  $k$ , and the energy for (b4) and (c4) is nearly degenerate.

#### Appendix D: Preparation of the initial state

The system is initially prepared in the odd parity state with barrier height  $d = 300$ , the wave function of which can be obtained through solving Eq. (A11) and Eq. (B1) for different interaction strength. The numerically computed quasi-momentums are  $k_1 = 2.734$  and  $k_2 = 3.6936$  for  $g = 0.5$ ,  $k_1 = 4.126$  and  $k_2 = 2.585$  for  $g = 1.5$ , and  $k_1 = 2.872$  and  $k_2 = 5.726$  for  $g = 20$ . These  $k_1$  and  $k_2$  are plugged into Eq. (2) to get the corresponding wave function for the

TABLE I: The weight coefficients  $C_i$ 

$C_i$	$g = 0.5$	$g = 1.5$	$g = 20$	$C_i$	$g = 0.5$	$g = 1.5$	$g = 20$
$C_1$	-0.8731618	0.8524551	0.666279	$C_{16}$	0.0000835	0.0001781	-0.00021
$C_2$	0.46679	-0.499186	-0.66614	$C_{17}$	-0.0328012	0.0338401	0.024499
$C_3$	-0.0188581	0.0534258	-0.24749	$C_{18}$	0.0007173	0.0021096	-0.00839
$C_4$	0.010067	0.0292036	-0.1765	$C_{19}$	-0.0001443	-0.000379	-0.00032
$C_5$	-0.1179361	0.1204126	0.065573	$C_{20}$	-0.0000502	-0.000114	-0.000057
$C_6$	-0.0024673	-0.0066555	-0.01626	$C_{21}$	-0.0007583	0.0022915	0.0193
$C_7$	0.0040574	0.0119879	0.069451	$C_{22}$	-0.0004255	-0.0014146	-0.01899
$C_8$	0.0022943	0.0074603	0.061807	$C_{23}$	0.0000968	0.0002537	-0.00169
$C_9$	0.000471	0.0010114	-0.00419	$C_{24}$	0.0000447	0.0001115	-0.00017
$C_{10}$	0.0558227	0.0573916	0.036043	$C_{25}$	0.0000239	0.0000509	-0.000025
$C_{11}$	0.0012207	-0.0035508	-0.01138	$C_{26}$	0.0216447	-0.02237	-0.01812
$C_{12}$	-0.0002296	0.000539	0.000308	$C_{27}$	-0.0004727	-0.0013925	-0.00643
$C_{13}$	-0.0015487	-0.0046468	-0.03337	$C_{28}$	0.0000958	0.0002573	0.000285
$C_{14}$	-0.0008721	0.0028878	0.031884	$C_{29}$	-0.0000357	-0.0000915	-0.000068
$C_{15}$	0.0001965	0.0004967	-0.00269	$C_{30}$	-0.0000161	-0.0000359	-0.000017

initial state, which can be regarded as the *NOON* state. Then we lower the barrier height from  $d = 300$  to  $d = 0.5$  and let the system to evolve with time. Therefore we choose the eigenstates with barrier height  $d = 0.5$  as a complete set, upon which the initial state is expanded. Here we only choose 30 eigenstates, since the weight coefficients  $C_i$  are very small when  $i > 30$ , which are shown in the Table. I